Theoretical study of [111]-germanium nanowires as anode materials in rechargeable batteries: a density functional theory approach

R. Jiménez-Sánchez[a], P. Morales Vergara[a], F. Salazar[a], A. Miranda[a], A. Trejo[a], I. J. Hernández-Hernández[b], L. A. Pérez[b], and M. Cruz-Irisson[a]

[a]*Instituto Politécnico Nacional, ESIME-Culhuacan, Av. Santa Ana 1000, 04430, Ciudad de México, México.*
[b]*Instituto de Física, Universidad Nacional Autónoma de México, Apartado Postal 20-364, 04510, Ciudad de México, México.*

Received 3 December 2022; accepted 10 January 2023

In this work, we present a density functional theory study of hydrogen-passivated germanium nanowires grown along the [111] crystallographic direction. The study is performed within the local density approximation and the supercell technique. Four different diameters of nanowires were considered and the surface hydrogen atoms were replaced by Li ones using a sequential process. The results indicate that the nanowires have a semiconductor behaviour and the energy band gap diminishes when the number of Li atoms per unit cell increases. The formation energy results reveal that the Li atoms increase the stability of the Ge nanowires, and there is a charge transfer from the Li atoms to the surface Ge atoms. The open-circuit voltage values are almost independent of the concentration of Li atoms. Moreover the lithium storage capacity results reveal that the Ge nanowires could be good candidates to be incorporated as anodic materials in the new generation of rechargeable batteries.

Keywords: Germanium nanowires; energy storage; anode materials; density functional theory.

DOI: https://doi.org/10.31349/RevMexFis.69.031604

1. Introduction

The understanding of the electronic properties of nanostructures allows the design of materials with specific features according to the required applications. The synthesis and the computational modeling of nanostructures are fundamental to understand, improve, and control their properties. The quantum confinement and the large surface of nanomaterials can be used to control their electronic properties [1]. Nanomaterials can have an important impact in diverse fields of medicine, communications, sensing, optoelectronic devices, pollution control, and energy storage devices including the renewable energy sources [1–11]. In particular, they can be used to fabricate supercapacitors and rechargeable batteries, such as the Li-ion batteries, which have large gravimetric capacities and low discharge ratios when the battery is not being used. Currently, the anodes in Li-ion batteries are made of graphite. These batteries have a specific energy capacity close to 380 mAh/g [12] and a power around 10^2 W/kg [13], which is still far from the 10^6 W/kg obtained from fossil fuels. Some semiconducting materials offer higher capacities to store Li, like crystalline Si and Ge with 4200 mAh/g and 1200 mAh/g, respectively [14, 15]. However, these materials have not been incorporated as anodes because the insertion of Li atoms in the crystal fractures the material after a few charge-discharge cycles, due to the internal tensions that the Li atoms produce in them. It has been shown that the free space between nanowires in a given array may diminish those internal stresses [16, 17]. Also, the nanowire structure constrains the electronic transport to one dimension. These results indicate that silicon or germanium nanowires could be used as anode materials. In particular, germanium has a working potential of 0.5 V respect to Li/Li^+ and its small gap makes it more electrically conductive in comparison with other semiconductor materials [18–20]. In addition, Ge nanowires are more stable and have larger Li storage capacities in comparison with Si nanowires [19]. Moreover, experimental reports indicate that the charge/discharge process in Ge-nanowire arrays results in a porous nanostructure with a high performance and a Coulomb efficiency around 100 % after 100 cycles [21]. Likewise, the growth of Ge nanowires using substrates of stainless steel, leads to capacities of 894 mAh/g after 250 charge/discharge cycles [22]. Also, it has been reported that carbonaceous germanium (C-Ge) nanowires, with diameters between 11 and 19 nm, still have specific energy capacities larger than 1200 mAh/g after 500 cycles [23]. On the other hand, the current computational power has reduced the gap between the experimental study of nanostructures and the corresponding theoretical results. Likewise, the computational modeling allows to control the physical and chemical environment of a given nanostructure. In particular, the chemical reactivity at the surface of pristine nanowires (dangling bonds) can be easily controlled through the hydrogen passivation process which also preserve the crystalline structure of the nanowire and maintain its semiconducting behaviour [24]. This procedure has been successfully implemented at the experimental level in Si and Ge nanowires [25, 26]. In this work, we study the effect of the surface Li atoms on the electronic properties of Ge nanowires, formerly passivated with hydrogen atoms, grown

along the [111] crystallographic direction and with hexagonal cross sections with four different diameters. In particular, we studied their energy band gaps, formation energies, and the maximum theoretical Li storage capacities to address the possibility to use them as anode materials.

2. Model and calculation scheme

Infinitely long Ge nanowires (GeNWs) grown along the [111] crystallographic direction and with four different diameters, between 1nm and 2 nm, were considered. The nanowire unit cells have a vacuum space of at least five nanowire lattice constants along the direction perpendicular to the nanowire axis to avoid the interaction between the nanowire images produced by the periodic boundary conditions. The density functional calculations were performed within the local density approximation (LDA) as implemented in the SIESTA code [29]. Norm-conserving pseudopotentials [27], in their fully nonlocal form [28] and double-ζ s, p basis with a single d orbital, were used. Also, the real-space grid for numerical integration was defined by an energy cutoff of 150 Ry . The Brillouin zones were sampled with $1 \times 1 \times 4$ k-points for the geometrical optimizations and $1 \times 1 \times 24$ for the electronic band structure and density of states calculations, both within the Monkhorst-Pack scheme [32]. The Hellmann-Feynman forces between the atoms at the equilibrium geometry were lower than 2 meV/Å. The Ge pseudopotential was generated with the atomic valence-electron configuration s^2p^2 and with pseudopotential core radii $s(1.89)$, $p(1.89)$ and $d(1.89)$ (in atomic units). The suitability of the pseudopotential was verified by calculating the bond length and lattice constant of crystalline Ge, whose obtained values had an error lower than 0.8% with respect to the corresponding experimental values [30], The radius of the nanowire was obtained following the procedure given in Ref. [31]. Figure 1 shows the non relaxed structures of the unit cells of the GeNWs labeled as M1, M2, M3, and M4. The model considers the replacement of H atoms by Li ones in a sequential process, indicated by the numbers besides the Li atoms, in order to simulate a charging process. GeNWs with morphologies M1, M2, and M3 were reported in Ref. [33] and studied in this work to compare its properties with those obtained in this work for the morphology M4. The diameters of the optimized H-GeNWs are 7.4 Å (M1), 12.0 Å (M2), 16.6 Å (M3), and 20.4 Å (M4).

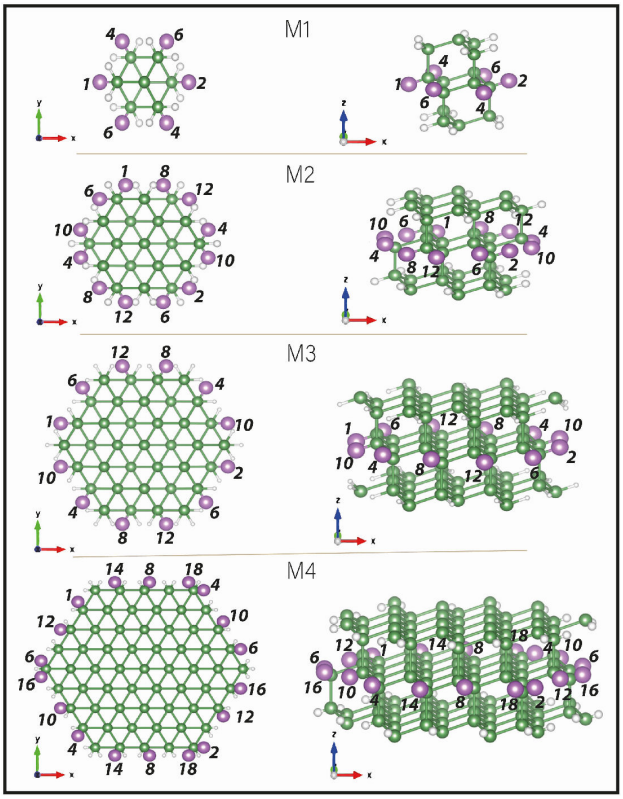

FIGURE 1. Cross sections and lateral views of the non relaxed morphologies of the four studied GeNWs labeled as M1, M2, M3, and M4. The numbers besides the Li atoms (violet spheres) indicate the sequence of substitution of H atoms (white spheres) by Li ones. The morphologies M1, M2, and M3 were taken from reference [33]. The green spheres represent Ge atoms.

3. Results and discussion

Figure 2 shows the electronic band structure of the M4 GeNW with three different concentrations of Li atoms per unit cell, (a) 2 Li, (b) 10 Li, and (c) 18 Li. At the right side of each electronic band structure, the densities of electronic states (DOS) per atomic species and the total density of states are depicted. The main contribution of the Li atoms occurs at the conduction bands, for the case of 2 Li atoms, see Fig. 2a). Likewise, the hydrogen atoms contribute with more states at the valence and conduction bands in comparison with the contribution of the Li ones. In contrast, for 10 Li atoms per unit cell, their contribution at the conduction bands is higher than that of the H ones (see Fig. 2b)) and for 18 Li atoms per unit cell, their contribution is noticeably larger than the H ones. For all the studied concentrations of Li atoms in

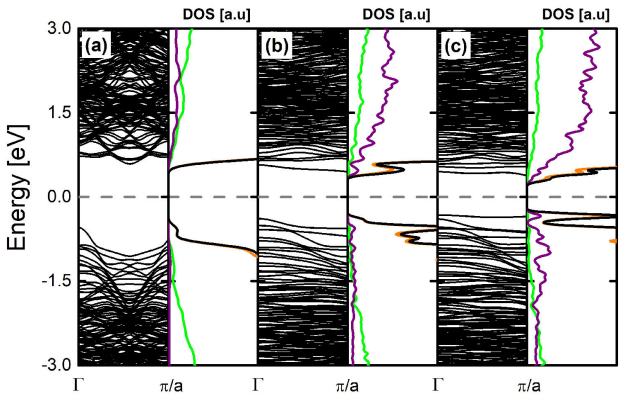

FIGURE 2. Electronic band structure, total density of electronic states (black lines), and densities of electronic states per species, Ge (orange), H (green), Li (violet), and total (black line), for the M4 Ge nanowire.

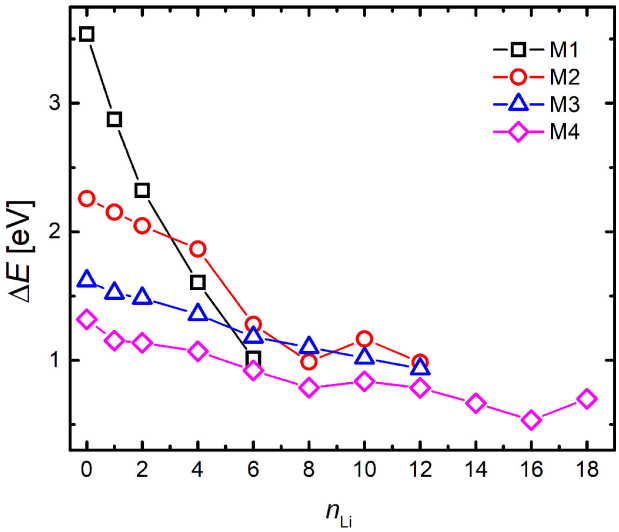

FIGURE 3. Energy band gap (ΔE) as a function of the number of Li atoms per unit cell ($n_{\rm Li}$) for the morphology M4 (pink diamonds) in comparison with the morphologies M1, M2, and M3 reported in Ref. [33].

the morphology M4, the nanowire maintains a semiconducting behaviour.

A general result is that all studied Ge nanowires with Li at the surface maintain a semiconducting behaviour, and the size of the band gap (ΔE) decreases when the diameter and the number of Li atoms per unit cell (n_{Li}) increases. The quantum confinement effect is more noticeable for the fully hydrogen-passivated GeNWs. Furthermore, the effect of the Li atoms is stronger than the quantum confinement effect for concentrations larger than 2 Li atoms per unit cell, as shown in Fig. 3, where ΔE for M1 is lower than that of M2 and M3, and has a similar value to that of M4 with $n_{Li} = 6$. The M4 GeNW has the lower values of ΔE in comparison with the other morphologies. According to previous theoretical studies which consider interstitial Li atoms in GeNWs, the nature of the semiconducting band gap has a strong dependence on the position of the Li atoms leading to both semiconducting or metallic behaviour [1], then the relevance of these results is that the GeNW considered in this work maintains a semiconducting behaviour for all the studied concentrations of surface Li atoms.

A Hirshfeld population analysis [34] for the M4 GeNW was performed. In particular, we calculated

$$\rho_x = \sum_{i=1}^{n_x} \rho_i^x, \qquad (1)$$

where ρ_x is the Hirshfeld electronic charge excess associated to the atom i, and n_x is the number of atoms of species $x =$ Ge, H or Li, per unit cell. Figure 4 shows the Hirshfeld electronic charge excesses, Eq. (1), on the different types of atoms as a function of the concentration of Li atoms. Observe that the Ge atoms lose electronic charge to form bonds with the H atoms at the surface of the nanowire, and the sum of both charge excesses is zero. For $n_{\rm Li} > 0$ the charge excess on Li atoms

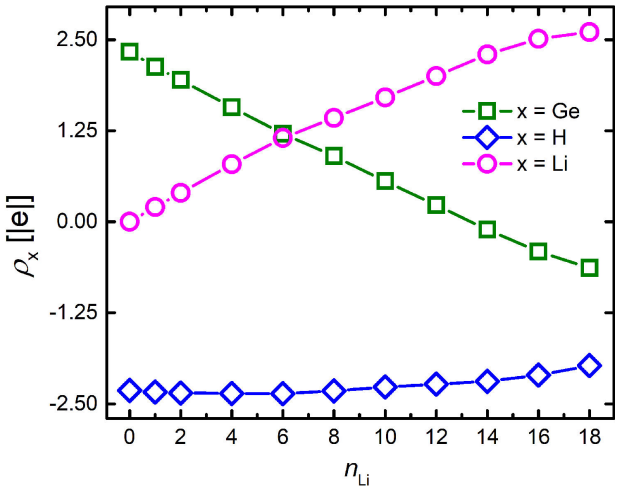

FIGURE 4. Hirshfeld charge excess per atomic species (ρ_x) as a function of the concentration of Li ($n_{\rm Li}$) atoms for the M4 GeNW.

(open pink circles) increases, while that of the Ge diminishes, indicating that the Li atoms transfer electronic charge to the surface Ge ones. It is worth to say that this behaviour was also observed for the morphologies M1, M2, and M3.

The energetic stability of the GeNWs was analyzed by calculating the formation energy which is given by

$$E_f(n_{\rm Li}) = \frac{1}{M}[E({\rm GeNW} + n_{\rm Li}) - n_{\rm Ge}E({\rm Ge_{bulk}}) - \frac{1}{2}n_{\rm H}E({\rm H_2}) - n_{\rm Li}E({\rm Li})], \qquad (2)$$

where M is the number of atoms in the unit cell, $E({\rm GeNW} + n_{\rm Li})$ is the energy of the nanowire with $n_{\rm Li}$ Li atoms, $n_{\rm Ge}$ and $n_{\rm H}$ are the number of Ge and H atoms per unit cell, $E({\rm Ge_{bulk}})$, $E({\rm Li})$ and $E({\rm H_2})$ are the energy of a single Ge atom in the bulk structure, the energy of one isolated Li atom,

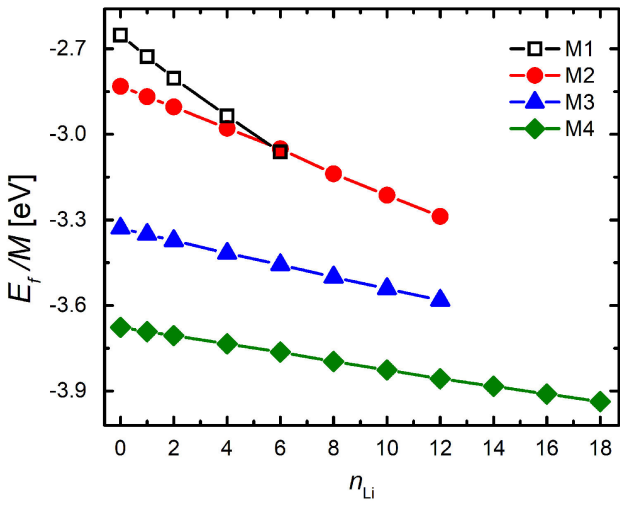

FIGURE 5. Formation energy of the GeNW with morphology M4 (green diamonds) as a function of the number of Li atoms per unit cell ($n_{\rm Li}$). The formation energies of GeNWs with geometries M1, M2, and M3 were taken from Ref. [33].

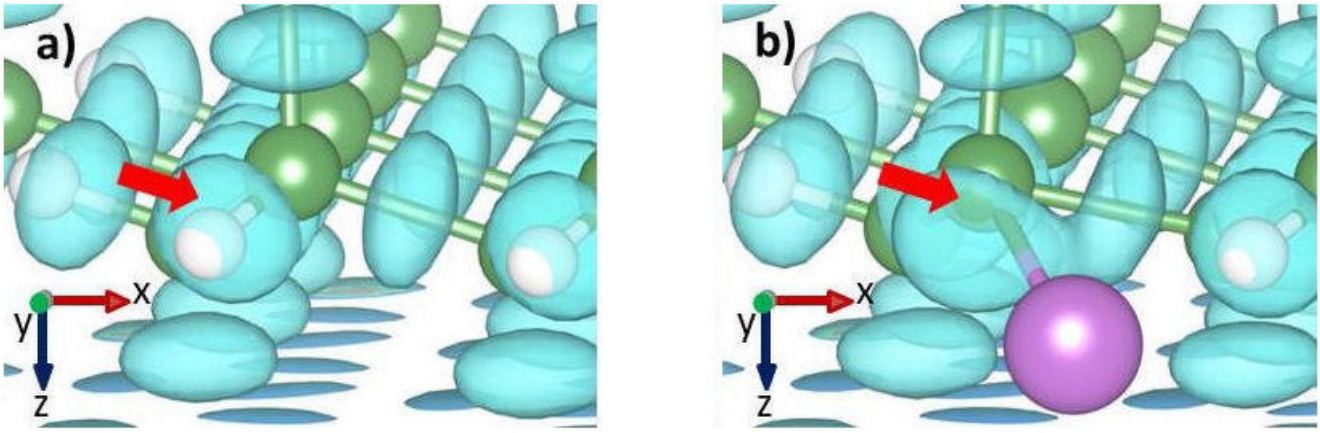

FIGURE 6. Charge density difference for a M4 GeNW a) fully-hydrogen passivated and b) with one Li atom per unit cell. The red arrow indicates the change of the charge density around the Ge atom when the H atom is replaced by a Li one.

and the energy of the H molecule, respectively. Observe that a negative value indicates a more energetically stable system. Figure 5 shows the formation energy as a function of the concentration of Li atoms per unit cell for the morphology M4 (green diamonds) in comparison with morphologies M1 (open black squares), M2 (red circles), and M3 (blue triangles) taken from Ref. [33]. Notice that the M4 GeNW is the more stable one.

To confirm the previous results of Figs. 4, and 5, we calculated the charge density difference given by

$$\delta\rho(\vec{r}) = \rho(\vec{r}) - \rho_{\text{atom}}(\vec{r}), \tag{3}$$

where $\rho_{\text{atom}}(\vec{r})$ is the charge density of the isolated atoms in the nanowire, and $\rho(\vec{r})$ is the charge density of the GeNW. Figure 6 depicts $\delta\rho(\vec{r})$ for the morphology M4 of the H-GeNW a) and the same region of the GeNW where one Li atom replaces a H atom b) for the isovalue 0.0321 $e\text{Å}^{-3}$, were it is possible to observe a spherical distribution of the charge density between the H and Ge atoms indicated with the red arrow. In contrast, the redistribution of the charge around the Li and Ge atoms in Fig. 6 b), indicated with the red arrow, confirms the Hirshfeld population analysis of Fig. 4.

The performance of GeNWs as electrodes can be estimated by calculating the open circuit voltage (OCV). Considering that the entropy and volume effects are negligible at 0 K [35], OCV is given by

$$OCV = \frac{\Delta_b}{|e|n_{\text{Li}}}, \tag{4}$$

where Δ_b is the binding energy, *i.e.*, the necessary energy to extract n_{Li} Li atoms per unit cell from the nanowire, and it is given by

$$\Delta_b(n_{\text{Li}}) = E(\text{H}-\text{GeNW}) + n_{\text{Li}}[E(\text{Li}) - \frac{1}{2}E(H_2)] - E(\text{GeNW}+n_{\text{Li}}), \tag{5}$$

where E(H-GeNW) is the energy of the fully-hydrogen passivated GeNW. Figure 7 shows OCV as a function of the concentration of Li atoms for M1 (black squares), M2 (red circles), M3 (blue triangles), and M4 (green diamonds) GeNWs. The results reveal that the voltage is almost independent of the concentration Li atoms for all studied GeNWs. This indicates that battery anodes based on GeNWs would offer a constant voltage, which is a very favourable situation for rechargeable batteries.

Likewise, the maximum lithium storage capacity C_M was obtained for the four morphologies of the studied GeNWs by using the following equation

$$C_M = \frac{z n_{\text{Li}} F}{M_{\text{GeNW}}}, \tag{6}$$

where z is the valence of the ionized atom ($z = 1$), F is the Faraday constant (26801 mAh/mol), and M_{GeNW} is the relative molecular mass of the Ge atoms in the unit cell.

Figure 8 shows C_M as a function of the concentration of Li atoms for all studied GeNWs. If we consider Li^- ions, values between 50 and 160 mAh/g were obtained. It is important to remember that the studied nanowires still have hy-

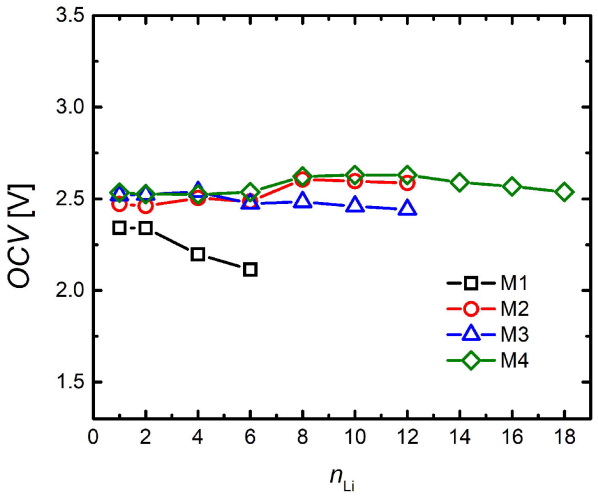

FIGURE 7. Open circuit voltage (OCV) of GeNWs with morphologies M1, M2, M3, and M4 as a function of the number of Li atoms per unit cell (n_{Li}).

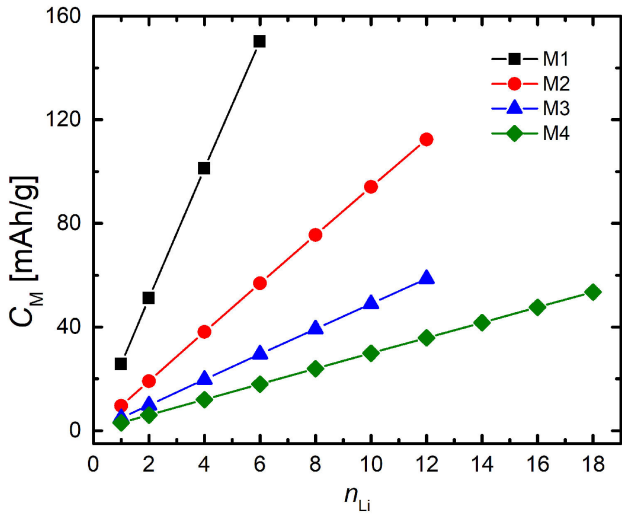

FIGURE 8. Maximum lithium storage capacity (C_M) of the studied GeNWs as a function of the concentration of Li atoms per unit cell (n_{Li}).

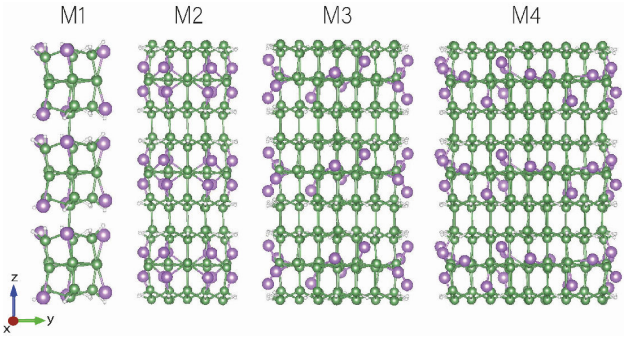

FIGURE 9. Lateral views of the structurally relaxed GeNWs with the maximum concentration of Li atoms studied.

drogen atoms that can be replaced by Li ones, then we expect higher values for these GeNWs. However, the Li atoms modify the nanowire structure as shown in Fig. 9, where the relaxed nanowires with the maximum concentration of Li atoms are depicted. It is worth to mention that the Li atoms at the surface of the nanowire barely modify the structure in comparison with nanowires with interstitial Li atoms [1].

4. Summary

In this work, we presented a density functional study of hydrogen-passivated GeNWs grown along the [111] crystallographic direction with different diameters and concentrations of substitutional Li atoms. The results indicate that electronic charge is tranferred from the Li atoms to the Ge ones at the surface of the nanowires. Likewise, the open circuit voltage values are almost constant for all studied GeNWs. Moreover, their lithium storage capacity is suitable for their use as anodic materials. These results allow to understand the effects of the Li atoms at the surface of Ge nanowires on their electronic and structural properties and open the possibility of tuning their properties in order to be used as energy storage devices.

Acknowledgements

This work was supported by IPN projects 2023-2074, and -2079, and UNAM-PAPIIT IN102923. The calculations were performed at the supercomputer Miztli of DGTIC-UNAM (project LANCAD-UNAM-DGTIC-180) and at Laboratorio Nacional de Supercómputo del Sureste de México (LNS) (project 20193082). R.J.S. acknowledges the financial support from CONACYT and IPN-BEIFI. I.J.H.-H. acknowledges the CONACyT posdoctoral scholarship given through the program "Estancias Posdoctorales por México". P.M.V. acknowledges the financial support from COTEPABE-IPN.

1. A. González-Macías *et al.*, Lithium effects on the mechanical and electronic properties of germanium nanowires, *Nanotechnology* **29** (2018) 154004, https://dx.doi.org/10.1088/1361-6528/aaaad4

2. S. Laumier *et al.*, Selection and Functionalization of Germanium Nanowires for Bio-Sensing, *ACS Omega* **7** (2022) 35288-35296, https://doi.org/10.1021/acsomega.2c04775

3. S. Singh *et al.*, $Ge - Ge_{0.92}Sn_{0.08}$ core-shell single nanowire infrared photodetector with superior characteristics for on-chip optical communication, *Appl. Phys. Lett.* **120** (2022) 171110, https://doi.org/10.1063/5.0087379

4. M. A. de Santiago, F. Pérez, L. A. Cruz-Irisson, Silicon nanowires as potential gas sensors: a density functional study, *Sens Actuators B.* **242** (2017) 1246-1250, https://doi.org/10.1016/j.snb.2016.09.085

5. A.N. Sosa *et al.*, Alkali and transition metal atom-functionalized germanene for hydrogen storage: A DFT investigation, *International Journal of Hydrogen Energy* **46** (2021) 20245-20256, https://doi.org/10.1016/j.ijhydene.2020.04.129

6. A. N. Sosa *et al.*, NH_3 capture and detection by metal-decorated germanene: a DFT study, *J. Mater. Sci.* **57** (2022) 8516-8529, https://doi.org/10.1007/s10853-022-06955-w

7. A. N. Sosa, I. González, A. Trejo, A. Miranda, F. Salazar, M. Cruz-Irisson, Effects of lithium on the electronic properties of porous Ge as anode material for batteries, *J. Comput. Chem.* **41** (2020) 2653- 2662, https://doi.org/10.1002/jcc.26421

8. L. G. Arellano *et al.*, Tunable electronic properties of silicon nanowires as sodium-battery anodes, *Int J Energy Res.* **46**

(2022) 17151- 17162, https://doi.org/10.1002/er.8378

9. P.H. Jariwala,Y.A. Sonavane, P.B. Thakor and Sanjeev and K. Gupta, Strain dependent electronic transport of pristine Si and Ge nanowires, *Computational Materials Science* **188** (2021) 110181, https://doi.org/10.1016/j.commatsci.2020.110181
10. H M Singh, B Choudhuri, and P Chinnamuthu, Investigation of Optoelectronic Properties in Germanium Nanowire Integrated Silicon Substrate Using Kelvin Probe Force Microscopy, *IEEE Transactions on Nanotechnology* **19** (2020) 628-634, https://ieeexplore.ieee.org/abstract/document/9145852
11. F. De Santiago et al., Lithiation effects on the structural and electronic properties of Si nanowires as a potential anode material, *Energy Storage Materials* **20** (2019) 438-445, https://doi.org/10.1016/j.ensm.2019.04.023
12. B. J. Landi, M. J. Ganter, and Cress, Cory D. and DiLeo, Roberta A. and Raffaelle, Ryne P., Carbon nanotubes for lithium ion batteries, *Energy Environ. Sci.* **2** (2009) 638-654, http://dx.doi.org/10.1039/B904116H
13. M. Stanley Whittingham, Materials Challenges Facing Electrical Energy Storage, *MRS Bulletin* **33** (2008) 411, https://doi.org/10.1557/mrs2008.82
14. A. S. Aricò Bruce, P. B. Scrosati, J. M. Tarascon, and W. Van Schalkwijk Nanostructured materials for advanced energy conversion and storage devices, *Nat. Mater.* **4** (2005) 366-77, https://doi.org/10.1038/nmat1368
15. N. Liu, W. Li, M. Pasta and Y. Cui, Nanomaterials for electrochemical energy storage, *Front. Phys.* **9** (2014) 323-50, https://doi.org/10.1007/s11467-013-0408-7
16. S. Wu *et al.*, Germanium-based nanomaterials for rechargeable batteries, *Angew. Chem. Int. Ed.* **55** (2016) 7898-922, https://doi.org/10.1002/anie.201509651
17. C. K. Chan, X. F. Zhang and Y. Cui, High capacity Li ion battery anodes using Ge nanowires, *Nano Lett.* **8** (2008) 307-9, https://doi.org/10.1021/nl0727157
18. C. Y. Chou and G. S. Hwang, On the origin of anisotropic lithiation in crystalline silicon over germanium: a first principles study, *Appl. Surf. Sci.* **323** (2014) 78-81, https://doi.org/10.1016/j.apsusc.2014.08.134
19. X. H. Liu *et al.*, In situ TEM experiments of electrochemical lithiation and delithiation of individual nanostructures, *Adv. Energy Mater.* **2** (2012) 722-41, https://doi.org/10.1002/aenm.201200024
20. J. Graetz, C. C. Ahn, R. Yazami and B. Fultz, Nanocrystalline and thin film germanium electrodes with high lithium capacity and high rate capabilities, *J. Electrochem. Soc.* **151** (2004) A698-702, https://iopscience.iop.org/article/10.1149/1.1697412
21. T. Kennedy, E. Mullane, H. Geaney, M. Osiak, C. O'Dwyer and K. M. Ryan, High-performance germanium nanowire-based lithium-ion battery anodes extending over 1000 cycles through in situ formation of a continuous porous network, *Nano Lett.* **14** (2014) 716-23, https://doi.org/10.1021/nl403979s
22. McNulty, D. Biswas, S. Garvey, S. O'Dwyer, C. Holmes, D. Justin, Directly Grown Germanium Nanowires from Stainless Steel: High-performing Anodes for Li-Ion Batteries, *ACS Appl. Energy Mater.* **3** (2020) 11811-11819, https://dx.doi.org/10.1021/acsaem.0c01977
23. A. Garcia *et al.*, One-Step Grown Carbonaceous Germanium Nanowires and Their Application as Highly Efficient Lithium-Ion Battery Anodes, *ACS Appl. Energy Mater.* **5** (2022) 1922-1932, https://doi.org/10.1021/acsaem.1c03404
24. R. Rurali, Colloquium: Structural, electronic, and transport properties of silicon nanowires, *Rev. Mod. Phys.* **82** (2010) 427, https://doi.org/10.1103/RevModPhys.82.427
25. Young-Dae Ko *et al.*, Sn-induced low-temperature growth of Ge nanowire electrodes with a large lithium storage capacity, *Nanoscale* **3** (2011) 3371-3375, https://doi.org/10.1039/C1NR10471C
26. T. Hanrath and B. A. Korgel, Nucleation and Growth of Germanium Nanowires Seeded by Organic Monolayer-Coated Gold Nanocrystals, *J. Am. Chem. Soc*. **124** (2002) 1424-1429, https://doi.org/10.1021/ja016788i
27. N. Troullier and J.L. Martins, Effient pseudopotentials for plane-wave calculations, *Phys. Rev. B* **43** (1991) 1993-2006, https://doi.org/10.1103/PhysRevB.43.1993
28. L. Kleinman and D.M. Bylander, Efficacious form for model pseudopotentials, *Phys. Rev. Lett.* **48** (1982) 1425-1428, https://doi.org/10.1103/PhysRevLett.48.1425
29. J.M. Soler *et al.*, The SIESTA method for ab initio order-N materials simulation, *J. Phys. Condens. Matter* **14** (2002) 2745, https://doi.org/10.1088/0953-8984/14/11/302
30. C. Kittel, Introduction to Solid State Physics, 7th ed. (John Wiley & sons, New York,1996), pp. 23.
31. F. Salazar and L. A. Pérez, Theoretical study of electronic and mechanical properties of GeC nanowires, *Comput. Mater. Sci.* **63** (2012) 47-51, https://doi.org/10.1016/j.commatsci.2012.05.066
32. H. J. Monkhorst, J. D. Pack, Special points for Brillouin-zone integrations, *Phys Rev B.* **13** (1976) 5188-5192, https://doi.org/10.1103/PhysRevB.13.5188
33. L. G. Arellano, F. Salazar, A. Trejo Baños, A. Miranda, L. A. Pérez and M. Cruz-Irisson, Electronic properties of [111] hydrogen passivated Ge nanowires with surface substitutional lithium, *IOP Conf. Series: Materials Science and Engineering* **840** (2020) 012004, https://dx.doi.org/10.1088/1757-899X/840/1/012004
34. C. Fonseca Guerra, J. W. Handgraaf, E. J. Baerends, F. M. Bickelhaupt, Voronoi deformation density (VDD) charges: assessment of the Mulliken, Bader, Hirshfeld, Weinhold, and VDD methods for charge analysis, *J. Comput. Chem.* **25** (2004) 189-210, https://doi.org/10.1002/jcc.10351
35. X. He, A. Tang, Y. Li, Y. Zhang, W. Chen and S. Huang, Theoretical studies of SiC van der Waals heterostructures as anodes of Li-ion batteries, *Appl Surf Sci.* **563** (2021) 150269, https://doi.org/10.1016/j.apsusc.2021.150269